

NUMERICAL SIMULATION OF AIR-LIFT PUMP

A thesis submitted in partial fulfillment of the requirements for the degree

of

Bachelor of Technology

in

Mechanical Engineering

by

Vivek Manna (Roll No. 111ME0310)

under the guidance of

Dr. Suman Ghosh



**DEPARTMENT OF MECHANICAL ENGINEERING
NATIONAL INSTITUTE OF TECHNOLOGY ROURKELA**

JUNE, 2015

© 2015 Vivek Manna. All rights reserved



CERTIFICATE

This is to certify that the thesis entitled “Numerical Simulation of Air-lift Pump”, submitted by Vivek Manna (Roll Number: 111ME0310) to National Institute of Technology, Rourkela, is a record of bona fide research work under my supervision, to the best of my knowledge in partial fulfilment of the requirements for the degree of Bachelor of Technology in the Department of Mechanical Engineering, National Institute of Technology Rourkela.

Place: Rourkela

Date:

Dr. Suman Ghosh
Assistant Professor
Department of Mechanical Engineering
National Institute of Technology Rourkela
Rourkela-769008, Odisha, India.

DECLARATION

I certify that

- 1) The work contained in the thesis is original and has been done by myself under the general supervision of my supervisor(s).
- 2) The work has not been submitted to any other Institute for any degree or diploma.
- 3) I have followed the guidelines provided by the Institute in writing the thesis.
- 4) I have conformed to the norms and guidelines given in the Ethical Code of Conduct of the Institute.
- 5) Whenever I have used materials (data, theoretical analysis, and text) from other sources, I have given due credit to them by citing them in the text of the thesis and giving their details in the references.
- 6) Whenever I have quoted written materials from other sources, I have put them under quotation marks and given due credit to the sources by citing them and giving required details in the references.

Date:
Place:

Signature of the Student
Vivek Manna (111me0310)

ACKNOWLEDGMENT

I would like to express my gratitude to my supervisor Dr. Suman Ghosh for his support during this project. I am exceedingly thankful to him for giving me this opportunity to work with him and for believing in me throughout the course of completion of this project. His valuable advice and persistent encouragement have helped me a lot to complete my project work successfully. Working under him was indeed a pleasure and inspiration for me.

I also like to thank the staff of Mechanical Department for providing me necessary amenities to finish this project.

Last but not the least, I would like to express my profound gratitude to God and my parents for their blessings without which this task could never have been accomplished.

VIVEK MANNA

Roll Number: 111me0310

CONTENTS

Title Page	i
Certificate by the Supervisors	ii
Declaration by the student	iii
Acknowledgement	iv
Contents	v
List of Figures	vii
List of Equation	viii
List of Symbols	viii
List of Abbreviations	viii
Abstract	ix
Chapter 1 Introduction and Literature Review	1
1.1 Introduction	2
1.2 Literature Review	4
1.3 Gaps in Literature	5
1.4 Aims and Objective	6
Chapter 2 Problem Statement	7
2.1 Problem Description	8
2.1.1 Effect of Air Mass Flow Rate on the Flow Regime	9
2.1.1.1 Air Inlet Mass Flow Rate = 0.0033 kg/sec.	9
2.1.1.2 Air Inlet Mass Flow Rate = 0.0110 kg/sec.	9
2.1.1.3 Air Inlet Mass Flow Rate = 0.0330 kg/sec.	9
2.1.2 Effect of Air Mass Flow Rate on Velocity of the Bubbles	10
2.1.3 Effect of Air Mass Flow Rate on Water Mass Flow Rate at Exit	10
Chapter 3 Methodology	11
3.1 Numerical Modelling	12

3.2 Governing Equation	13
3.3 Geometry and Grid Specification	14
3.4 Boundary Conditions	16
3.5 Solution Methods	16
3.6 Residuals	17
3.7 Values of Parameters for Simulation	17
Chapter 4 Results and Discussion	18
4.1 Grid Independence	19
4.2 Validation	21
4.3 Effect of Air Mass Flow Rate on the phenomenon	23
4.3.1 Effect of Air Mass Flow Rate on the Flow Regime	23
4.3.1.1 Inlet Mass Flow rate of air: 0.0033 kg/sec.	23
4.3.1.2 Inlet Mass Flow rate of air: 0.011 kg/sec.	27
4.3.1.3 Inlet Mass Flow rate of air: 0.033 kg/sec.	30
4.3.2 Effect of Air Mass Flow Rate on the Bubble Velocity	34
4.1.3 Effect of Air Mass Flow Rate on Water Mass Flow Rate at Exit	37
Chapter 5 Conclusion and Scope of Future Work	38
5.1 Conclusion	39
5.2 Scope of Future Work	39
References	41

LIST OF FIGURES

Figure no.	Title	Page no.
2.1	Schematic of the problem	9
3.1	Representation of geometry of Air-lift pump	15
3.2	Representation of mesh with 40000 nodes describing Air-lift pump	15
4.1	Variation of volume fraction of air at outlet with nodes for the AMFR of 0.033 kg/sec	20
4.2	Flow regime corresponding to four different mesh size at time $t = 1.0$ sec	20
4.3	Validation of bubbly flow	21
4.4	Validation of bubbly-slug flow	21
4.5	Validation of slug flow	22
4.6	Validation of slug-churn flow	22
4.7	Flow regime in the up riser pipe of ALP from time $t = 0.0$ sec to $t = 12.0$ sec with AMFR of 0.0033 kg/sec	26
4.8	Flow regime in the up riser pipe of ALP from time $t = 0.0$ sec to $t = 12.0$ sec with AMFR of 0.011 kg/sec	30
4.9	Flow regime in the up riser pipe of ALP from time $t = 0.0$ sec to $t = 12.0$ sec with AMFR of 0.033 kg/sec	33
4.10	Variation of bubble velocity with flow time for different air mass flow rate. (a) AMFR: 0.0033 kg/sec. (b) AMFR: 0.011 kg/sec. (c) AMFR: 0.033kg/sec.	35
4.11	Variation of AMFR with water mass flow rate at exit when submergence ratio is 0.4	36

LIST OF EQUATIONS

Equations	Page no.
Equation 3.1: Volume fraction equation	13
Equation 3.2: Continuity equation	13
Equation 3.3: Momentum equation	13
Equation 3.4: Turbulent kinetic energy equation	13
Equation 3.5: Turbulent dissipation energy equation	14
Equation 4.6: Velocity Mathematical definition	36

LIST OF SYMBOLS

Symbols	
ρ	Density(kg/m ³)
\vec{v}	Velocity(m/s)
p	Pressure(Pa)
\vec{g}	Gravity(m/s ²)
α	Volume fraction
m_{pq}	Transfer of mass from phase p to q
m_{qp}	Transfer of mass from phase q to p

LIST OF ABBREVIATIONS

Abbreviations	
ALP	Air-Lift Pump
AMFR	Air mass flow rate

ABSTRACT

Now a days, it is a basic necessity to have a very highly reliable pump with low maintenance. Moreover, for pumping of various kind of fluid like corrosive, abrasive, or even radioactive, an air-lift pump is very much useful. The only negative point of the ALP is that it has very low efficiency. Therefore, the goal is to perform an exhaustive research to increase the performance of the air-lift pump.

The purpose of the present effort is to capture the performance of air lift pump when it is operated in different flow regimes. To fulfill this objective, an air-lift pump is designed and numerically simulated using commercial software ANSYS. The results produced have been validated with the experimental data and have found to be in accordance with it. The pump works under two-phase flow condition with air and water as the two phases. Simulations were performed by varying the air mass flow rates. It is inferred that AMFR played a dominant role in improving the pump's performance and efficiency. It is concluded that for obtaining a good efficiency in an ALP, it should be operated either in slug or slug-churn flow regime.

Keywords: Air-lift Pump, Volume of Fluid (VOF), Finite Volume Method (FVM), Two Phase Flow, Volume Fraction, Numerical Modeling.

CHAPTER 1:

INTRODUCTION AND

LITERATURE REVIEW

In this chapter, a thorough introduction to an ALP is provided. Its necessity, its advantages and disadvantages have been discussed along with the literature review covering the work that has been done so far. Also, the gaps found in the literature have been mentioned and the aims and objectives of the present work has been described in accordance with the gaps found.

1.1 INTRODUCTION

With the decrease in the level of natural resources, we have started focusing on the sustainable use of natural resources and for achieving that there is a demand for highly reliable machinery with high efficiency and low operational costs. Having this in mind a great emphasis is being given to the development of ALP for water or oil pumping application. Even though these types of pumps have great advantages but still it's under developing stage, and an intensive research is required in this field before commercialization.

Air-lift pump is an equipment used for raising fluid mixture or mixture of fluid-solid through an up-riser pipe, partly filled with the liquid by injecting air at the bottom end of up-riser. The air then moves up along with the fluid. Its principle of operation is based on the buoyancy force exerted by air to liquid. Moreover, air added reduces the specific gravity of fluid mixture, and because it becomes lighter than surrounding liquid, it is pushed up. Since, an ALP works on liquid-air multiphase flow and is based on the aerating phenomenon. So, at this point a brief introduction to multiphase flow becomes necessary.

A multiphase flow is a simultaneous flow of more than one phase where their interface is influenced by their motion. Although a four phase simultaneous flow of liquid-solid mixture of water, sand, crude oil and gas is not so uncommon in oil exploration. But, a

two-phase flow mixture commonly occurs in many practical situations. Here, in our discussion we also have considered a two-phase flow regime consisting of air and water.

Air-lift pumps have significant advantages because of which it is more desirable than any other mechanical pumps. One such advantage is the absence of any mechanical transmission, which avoids any chances of hazardous activities like water hammer and other dynamic problems. Lack of impeller blade is an added advantage as it makes it useful for digging application, such as removing sediments from the riverbed and for mining precious minerals from the ocean floor. As there are no moving parts, there is a chance of minimal wear that reduces the need for maintenance and thus lowers the pumps cost and improves its reliability.

Moreover, these pumps could be used to transport slurries, corrosive or, toxins that could damage a mechanical pump. These pumps can even be used for the transfer of highly viscous hydrocarbons.

In spite of all these advantages, still air-lift pumps operate at significantly lower efficiencies than other mechanical pumps. Air-lift pumps typically operate in a low efficiency range of 35% to 40% whereas the mechanical pumps operate at much higher efficiency. Lower effectiveness in these pumps implies higher slip ratio between air and water as a result there is a reduced momentum transfer from gas to liquid. Due to this reduced efficiency problem, a rigorous study is required in this field. In our case, we are going to compare various flow regimes possible in two-phase air-lift pump consisting of air and water and based on study decide which flow regime is beneficial for achieving a higher efficiency level.

1.2 LITERATURE REVIEW

By 1882, researchers understood the working principle of an air-lift pump but the practical implementation of it didn't appear until the commencement of mid of the twentieth century. It was [Bergeles \(1949\)](#) who first studied the flow of the gas-liquid mixture experimentally. Later on, [Stenning and Martin \(1968\)](#) studied the performance of ALP and tried to understand the effect of pipe diameter, submergence and air flow rate on it.

[Sharma and Sachdeva \(1976\)](#) inspected the performance of bigger diameter air-lift pump when operated at narrow pits. They studied how the performance of the pump was effected by flow regime in up-riser. Then, [DeCachard and Delhaye \(1996\)](#) depicted experimentally that slug flow regime is dominant in a small size diameter pump when it ran practically.

A few studies were also conducted to explore the weightage of liquid property such as viscosity, surface roughness on the efficiency of ALP. For instance, [Khalil and Mansour \(1990\)](#) performed an experiment to investigate the impression of the addition of small amount of surfactant in liquid to be lifted. They concluded that when surfactants are used in small quantity it always improves pump's efficiency. [Iguchi and Terauchi \(2001\)](#) observed the outcome of pipe wall wettability in the transition from sluggish to bubbly flow regime and vice versa in a vertical pipe. For wettability, the pipe was coated with a hydrophilic substance. [Furukawa and Fukano \(2001\)](#) studied how viscosity effects the upward rising flow of two-phase flow in an up-riser pipe consisting of air and water. [Hitoshi et al. \(2003\)](#) found that point of injection plays a very crucial role on the discharge rate of water. He further showed through experimentation that as injection point of gas reaches above 45 times the up-riser diameter, then released water flow rate reduces. [White and Beardmore \(1962\)](#) and

[Zukoski \(1996\)](#) independently studied the influence of surface tension on the dynamics of up-riser slug flow when the pipe diameter was under 20 mm. [Kassab et al. \(2008\)](#) studied the characteristics of ALP under two-phase flow conditions. They performed experiments for all nine submergence ratios, also varied three riser length and later compared the experimental data with theoretically proposed model. They further concluded that ALP works efficiently in slug and slug-churn flow regimes.

Even though the geometry and the pump's working appear very simple but the theoretical study of this kind of pump is quite complex. The efforts to explain it began quite early in last century. Among the early classical theories of the ALP, some of them were presented by Harris, Lorenz as mentioned by [Stapanoff \(1929\)](#). Harris took into account the force of buoyancy and analyzed the motion of bubble. He believed that buoyancy force is mainly responsible for the working of pump, and he even obtained a relation between bubble size, slip (velocity of a bubble of air relative to water) and discharge head. Lorenz used Bernoulli's equation and applied its principle for an infinitesimally small head for the flow in up-riser. [Stapanoff \(1929\)](#) studied the effect of submergence, air to water ratio on the efficiency from the thermodynamic point of view. Later on, in 1963 a theoretical approach to study the ALP, based on sluggish flow working on two-phase was presented by [Nicklin \(1963\)](#).

1.3 GAPS IN LITERATURE

As can be seen from literature review that today, we have immense knowledge on two-phase flow type air-lift pumps. But, most of the work performed so far involves either an experimental approach or a theoretical approach to model an air-lift pump. But, only a few has been carried on this topic by numerical simulation to the best of the author's knowledge. One of them is [Hanafizadeh et al \(2009\)](#) where the effect of bubble size

and tapered diameter of up-riser pipe on performance of air-lift pump has been studied. Later [Hanafizdeh et al \(2014\)](#) also studied gas lift phenomenon using both VOF and Eulerian method. Moreover, as large resources are required for experimental setup of an air-lift pump and as it very time consuming and costly affair, one can go for numerical simulation.

1.4 AIMS AND OBJECTIVE

In the present study, effect of different flow regimes on the performance of an air-lift pump will be investigated. Here, flow rate is being varied to achieve various flow pattern like a slug, bubbly, annular and churn flow condition for same submergence ratio. Moreover, conversion of flow regimes were also witnessed and results were argued taking flow regime into account. We also aim to observe the effect of air mass flow rate on air bubble velocity and water mass flow rate at the exit of the up-riser.

CHAPTER 2:

PROBLEM

DESCRIPTION

In this chapter a detailed description of the problem is being discussed along with the effect of various parameter on it.

2.1 PROBLEM DESCRIPTION

Problem's schematic is shown in Figure 2.1. The setup consists of (A) a vertical up-riser pipe of length (L) 375 cm and diameter 2.54 cm, a down-comer (B) of diameter 2.54 cm and a riser (C) pipe of length 150 cm and diameter 2.54 cm. The water is fully filled and maintained in the riser pipe up to a height ($H_s = 150$ cm) and it is required to raise the air-water mixture up to a height of 375 cm. Thus, submergence ratio (ratio of up-riser length to immersed length) equal to 0.4. Air enters the up-riser pipe through a circumferential channel of height 5 cm affixed at a height of 25 cm from the down comer's end.

For numerical simulation, it is assumed that flow is 2D in nature, and simulation are performed in the unsteady state with a time step of 0.0001. Moreover, the air inlet is made mass-inlet type whereas, water inlet is made pressure-inlet type, and water-air outlet is made pressure-outlet type ($P_{atm} = 1.01325 \times 10^5$ Pa). At outlet pressure is assumed to be atmospheric. Wall is defined using no slip and no penetration boundary condition. Moreover, there is no heat transfer across the wall. A two-phase flow of air and water is flowing through the up-riser.

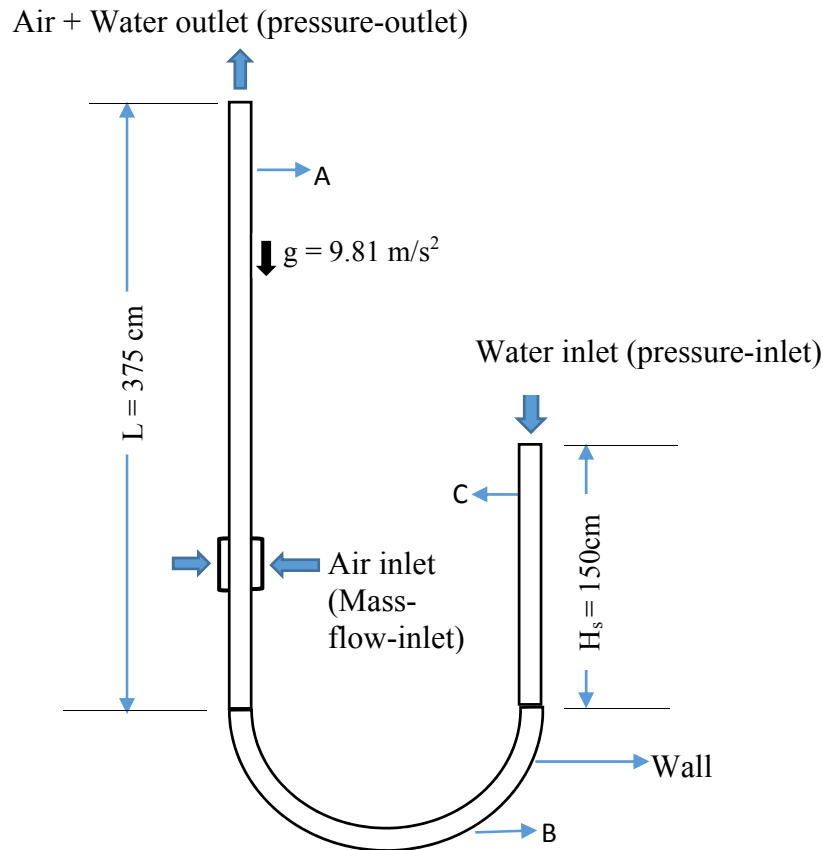


Figure 2.1: Schematic of the problem. A- Up-riser pipe; B- Down-comer; C- Riser.

2.1.1 Effect of Air Mass Flow Rate on Flow Regime

In this section the influence of AMFR on the flow regimes is being studied. Here, three AMFR are being varied and its effects will be shown in Chapter 4.

2.1.1.1 Air inlet mass flow rate = 0.0033 kg/sec: Here, AMFR is set to a value of 0.0033 kg/sec.

2.1.1.2 Air inlet mass flow rate = 0.0110 kg/sec: Here, AMFR at the inlet is increased to the value of 0.0110 kg/sec.

2.1.1.3 Air inlet mass flow rate = 0.0330 kg/sec: The AMFR is further increased to the value of 0.0330 kg/sec.

2.1.2 Effect of Air Mass Flow Rate on Velocity of the Bubbles

Here, the velocity of bubble is being calculated by varying the AMFR at inlet and its influence on bubble's velocity is further discussed in Chapter 4.

2.1.3 Effect of Air Mass Flow Rate on Water Mass Flow Rate at Exit

In this section, the AMFR is changed and its effect on Water Mass Flow Rate at the outlet is being studied. A detailed discussion is provided in Chapter 4.

CHAPTER 3:

METHODOLOGY

In this chapter, the methodology adopted for the present study is extensively explained. To numerically simulate the problem, Finite Volume Method (FVM) with Volume of Fluid Model (VOF) has been used. 2D unsteady analysis have been performed to capture the flow regime (flow structure) properly. Commercial CFD software Fluent in ANSYS 15 has been used to numerically simulate the problem.

3.1 NUMERICAL CALCULATION

In the present study, Volume of Fluid (VOF) model has been used to numerically simulate the two-phase flows in an upright pipe. The VOF model is used to solve the multiphase problem that involves mixtures of two or more immiscible fluid by continuity and momentum equation and keeps the record of the volume fraction of each fluid throughout the whole system. It can be quite accurately used for both 2D as well as 3D geometry. Tracking large bubbles in liquid mixture and tracking of steady or transient fluid-gas interface are some of its major application. It depends on the fact that two or more phases don't interpenetrate. For modelling of phases it adds additional volume fraction functions to the computational cells of control volume. So, the volume fraction of each fluid comes into play to determine field variables and properties. Based on all above mentioned advantages for simulating a multiphase flow, VOF was used. Moreover, it was also suggested by Hanafizdeh et al., 2009 in his Journal that for bubbly and slug flow VOF is most suited. Whereas, for annular, Eulerian is more appropriate. For turbulence modelling, standard $k-\varepsilon$ model is used. The Standard $k-\varepsilon$ is the most commonly used turbulence model. It is robust and reasonably precise for a wide range of application. For near wall treatment standard wall function has been used.

3.2 GOVERNING EQUATIONS

The governing equations used are shown below. Here, volume fraction α for each phase such that

$$\sum_{i=1}^n \alpha_i = 1 \quad (3.1)$$

where, n is number of phases involved in the problem.

Continuity Equation:

For i^{th} phase

$$\frac{1}{\rho_i} \left[\frac{\partial(\alpha_i \rho_i)}{\partial t} + \nabla \cdot (\alpha_i \rho_i \vec{v}_i) \right] = \sum_{i=1}^n (\dot{m}_{pq} - \dot{m}_{qp}) \quad (3.2)$$

Where, α_i , \vec{v}_i and ρ_i are volume fraction, velocity and density for i^{th} phase respectively

Since, mass transfer between air and water is zero, which implies that $\dot{m}_{pq} = \dot{m}_{qp} = 0$.

Momentum Equation:

Unlike continuity equation, in momentum equation only is first solved for the whole system and then computed velocity is distributed amid the phases present. The momentum equation dependent on all phases is given as:

$$\frac{\partial(\rho \vec{v})}{\partial t} + \nabla \cdot (\rho \vec{v} \vec{v}) = -\nabla p + \nabla \cdot (\mu(\nabla \vec{u} + \nabla \vec{u}^T)) + \rho \vec{g} + \vec{F} \quad (3.3)$$

Turbulence modelling using *k-epsilon* equation:

Turbulence kinetic energy k equation is used to determine the turbulence velocity scale:

$$\frac{\partial}{\partial t}(\rho k) + \frac{\partial}{\partial x_i}(\rho k u_i) = \frac{\partial}{\partial x_j} \left[\left(\mu + \frac{\mu_i}{\sigma_k} \right) \frac{\partial k}{\partial x_j} \right] + G_k + G_b - \rho \varepsilon - Y_M + S_k \quad (3.4)$$

and Turbulence dissipation energy ε equation is given by

$$\frac{\partial}{\partial t}(\rho\varepsilon) + \frac{\partial}{\partial x_i}(\rho\varepsilon u_i) = \frac{\partial}{\partial x_j} \left[\left(\mu + \frac{\mu_t}{\sigma_\varepsilon} \right) \frac{\partial \varepsilon}{\partial x_j} \right] + C_{1\varepsilon} \frac{\varepsilon}{k} (G_k + C_{3\varepsilon} G_b) - C_{2\varepsilon} \rho \frac{\varepsilon^2}{k} + S_\varepsilon$$

(3.5)

where,

G_k = Generation of turbulence kinetic energy due to the mean velocity gradients.

G_b = Generation of turbulence kinetic energy due to buoyancy.

$C_{1\varepsilon}, C_{2\varepsilon}$ & $C_{3\varepsilon}$ = constants. σ_k & σ_ε = Turbulent Prandtl numbers.

S_k & S_ε = User-defined source terms.

$\mu_t = \rho C_\mu \frac{k^2}{\varepsilon}$ = The turbulent viscosity.

3.3 GEOMETRY AND GRID SPECIFICATION

The geometry of the given problem was created in a workbench. Firstly, y-z plane was selected and a 2D profile of air-lift pump was constructed. An up-riser pipe of length 375 cm connected to one end of U-bend tube and other end of it was connected to riser pipe of length 150 cm. All the connected tubes have the same diameter of 2.54 cm. For air inlet two symmetrical passages of length 5 cm were provided at the height of 25 cm from the U bend tube. From this basic frame, surface was created. The Grids have been prepared in Meshing Workbench. The mesh arrangement for 2D case consists of 41045 nodes. The Grids have been created by default meshing scheme. For Grid Independence test grids with 35000, 38000, 45000 nodes were also generated by varying the minimum edge size. Moreover, named selection was also provided to the different zones where later boundary condition are to be provided.

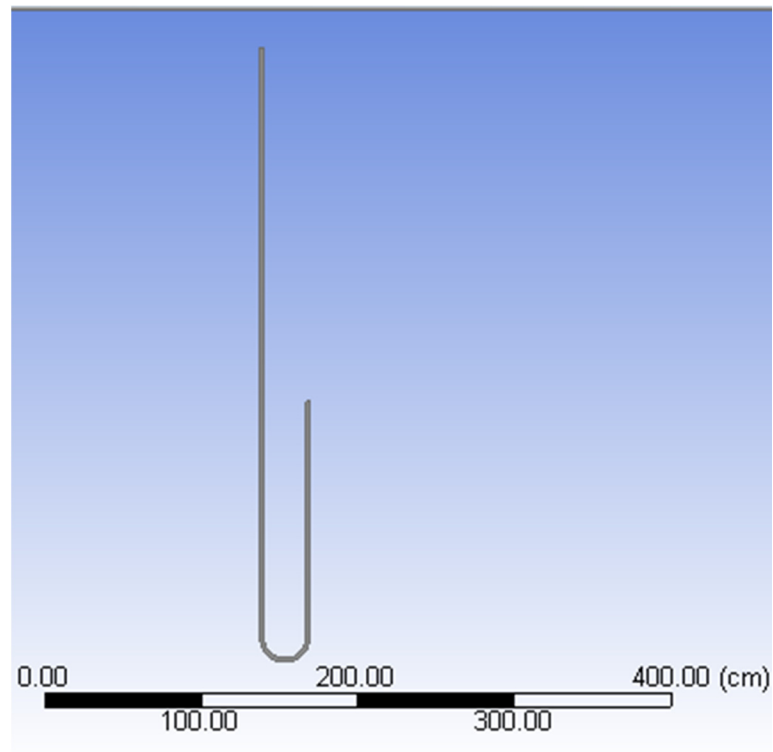


Figure 3.1: Representation of geometry of Air-lift pump

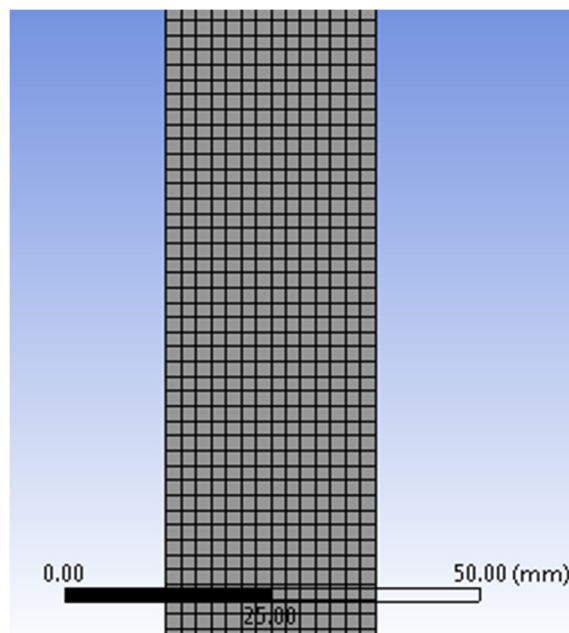


Figure 3.2: Representation of mesh with 40000 nodes describing Air-lift pump

3.4 BOUNDARY CONDITIONS

Boundary conditions provided here divides the whole geometry into different zones. For Air inlet, mass flow rate was enabled and then AMFR is varied for each case. Next zone is water inlet in which pressure-inlet was enabled. And, for maintaining a constant water level in riser pipe water volume fraction value, is set to unity. The next zone is a water-air mixture outlet from which two-phase mixture comes out. It is located at the top of up-riser pipe. To avoid any chances of reverse flow of air-water mixture the backflow volume fraction of water is set to zero. To account the effect of surface tension, the surface tension modelling was enabled, and a constant value of 0.072 was used.

3.5 SOLUTION METHOD

Here, 2D planar flow has been considered where the phenomena is transient. Pressure based solver is used. As the system is vertical, gravity is also considered. For turbulence modelling, standard k - ϵ model is used. The multiphase model has been enabled along with two-phases which were air and water. Air is considered as primary phase and water as a secondary phase. The pressure-velocity coupling is done by PISO scheme as it is strongly suggested for cases involving a transient flow, especially in case of large time step. As the mesh is not distorted, skewness and neighbor relaxation factors are set to unity. Under spatial discretization, Least Square Cell Based Gradient has been used. In this scheme, PRESTO for Pressure, GEO- CONSTRUCT for volume fraction have been used as suggested by Hanafizadeh et al., 2014. Moreover, first order upwind for both turbulent kinetic energy and Turbulent Dissipation Rate and second order upwind for momentum have been used. In Transient Formulation scheme, first order upwind is used.

3.6 RESIDUALS

Under Residuals, the Convergence criteria for all the field variables (continuity, x -velocity, y -velocity, k , and ε) are set to $1e-06$. Time stepping method is used as fixed type. The time step size is used as 0.0001 sec and maximum number of iteration per time step is set to 40. Reporting interval and profile update interval is set to unity. The case and data file are auto-saved with a regular interval of 0.2 sec.

3.7 VALUES OF PARAMETERS FOR SIMULATION

Turbulent kinetic energy $k = 3.260327 \times 10^{-12} \text{ m}^2/\text{s}^2$ and Turbulent dissipation rate $\varepsilon = 1.547478 \times 10^{-16} \text{ m}^2/\text{s}^3$. The fluid properties were set as: Density of water = 998.2 kg/m^3 , Viscosity of water = $0.001003 \text{ Pa}\cdot\text{s}$, Density of air = 1.225 kg/m^3 , viscosity of air = $1.7894 \times 10^{-5} \text{ Pa}\cdot\text{s}$. Values of the model constants: $C_{1\varepsilon} = 1.44$, $C_{2\varepsilon} = 1.92$, $C_{3\varepsilon} = 0.09$, $\sigma_k = 1$ & $\sigma_\varepsilon = 1.3$

CHAPTER 4:

RESULTS

AND

DISCUSSIONS

This section is devoted for conferring the results obtained after performing the numerical simulation of an air-lift pump by numerical simulation and attempts to discuss the various flow regimes observed and list probable causes of variation. It consists of sections describing grid independence and verification of numerical results. It also attempts to answer the probable effect of AMFR on flow regimes, bubble velocity, volume fraction of water at outlet and water mass flow rate at the outlet.

4.1 GRID INDEPENDENCE

Grid independence test is an important test which should be conducted before starting any analysis to validate the methodology. It is performed to avoid the influence of grids on the computational results. Here, grid independence test is carried out with the 2D air lift pump model. To perform this test, four different mesh structure with nodes 35000, 38000, 40000 and 45000 have been considered. Area weighted average volume fraction of air at the outlet at time $t = 2.0$ seconds for AMFR of 0.033 kg/sec is numerically calculated using each of these mesh arrangements. And ultimately they have been compared as shown in Figure 4.1. Moreover, the phase contours of flow regimes obtained for all the four meshes have been compared in Figure 4.2. From these Figures, it is clear that when the number of nodes is greater than 38,000, no substantial difference observed in the flow regimes or flow structures. Therefore mesh arrangement with 38,000 nodes is the minimum requirement to get correct results. Therefore in the present case, for numerical simulation mesh arrangement with 40,000 nodes has been considered.

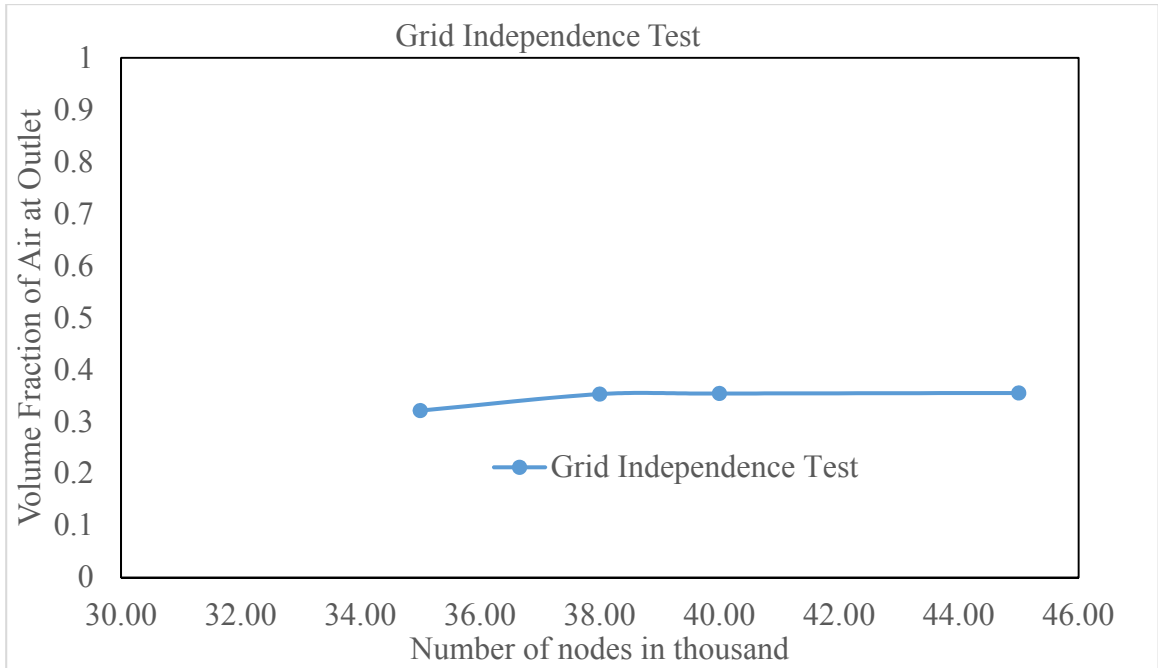


Figure 4.1: Variation of volume fraction of air at outlet with nodes for the AMFR of 0.033 kg/sec

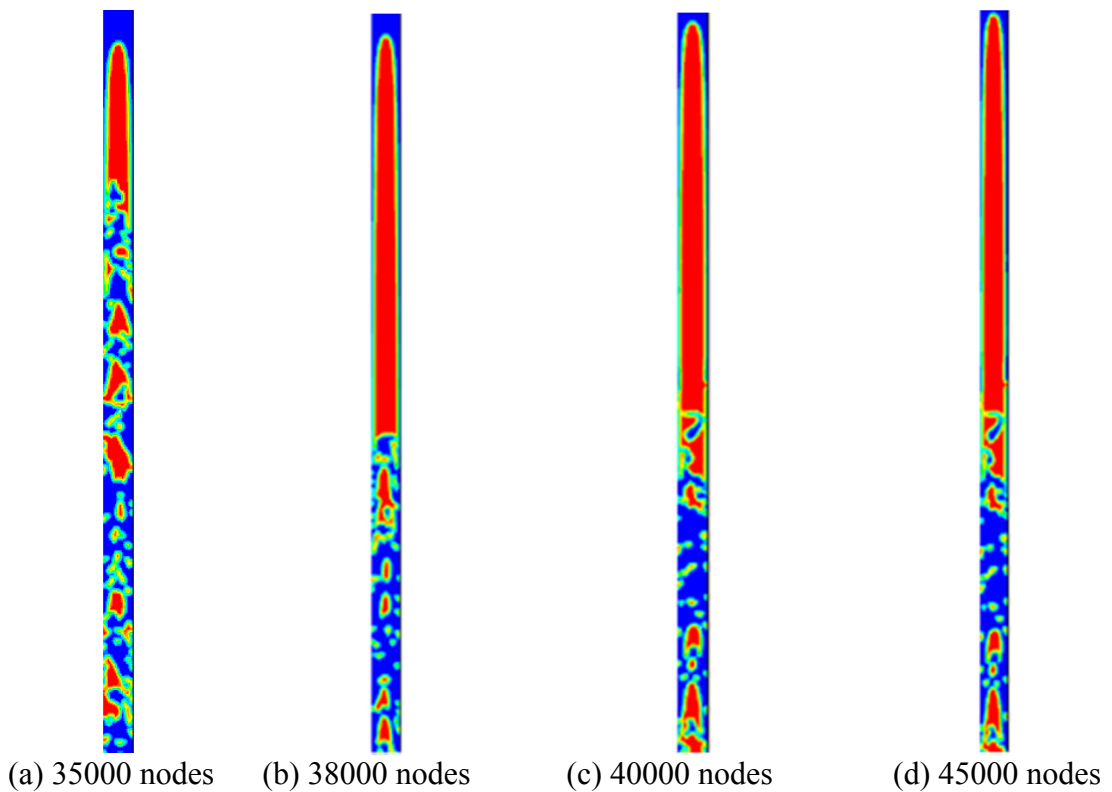


Figure 4.2: Flow regime corresponding to four different mesh size at time $t = 1.0$ sec

4.2 VALIDATION

Experimental validation is an important test which is conducted to confirm whether the results obtained from the numerical methods are similar to that obtained from experimentation. Here, validation has been performed by comparing numerical results obtained from the present methodology with the experimental results of [Kassab et al. \(2008\)](#). The validation results are categorically mentioned below.

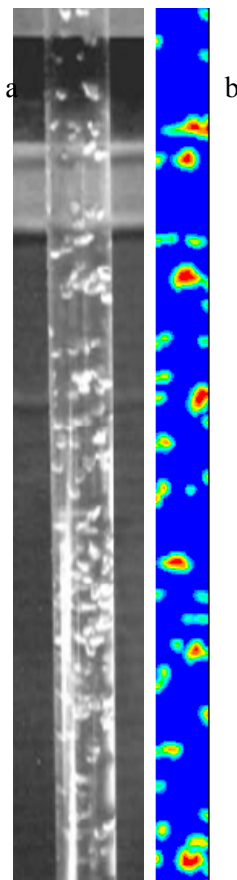


Figure: 4.3: Validation of Bubbly Flow, (a) bubbly flow from [Kassab et al. \(2008\)](#), (b) Simulation result for bubbly flow at time $t = 10$ sec where AMFR is 0.0033 kg/sec

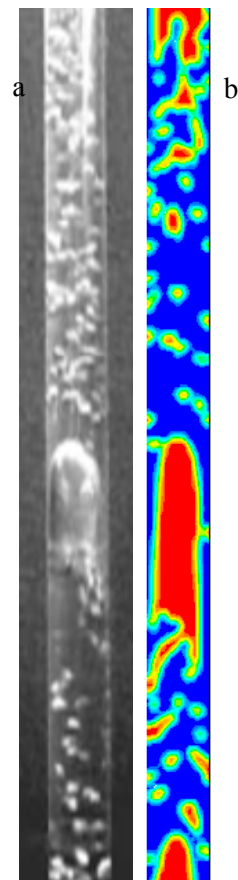


Figure: 4.4: Validation of Bubbly Flow, (a) bubbly-slug flow from [Kassab et al. \(2008\)](#), (b) Simulation result for bubbly flow at time $t = 10$ sec where AMFR is 0.033 kg/sec

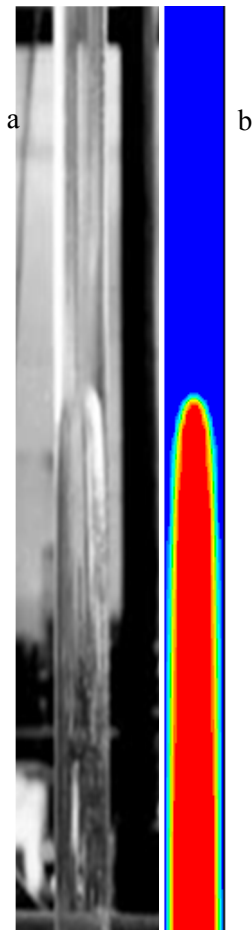


Figure: 4.5: Validation of Slug Flow, (a) slug flow from [Kassab et al. \(2008\)](#), (b) Simulation result for slug flow at time $t = 1$ sec where AMFR is 0.033 kg/sec

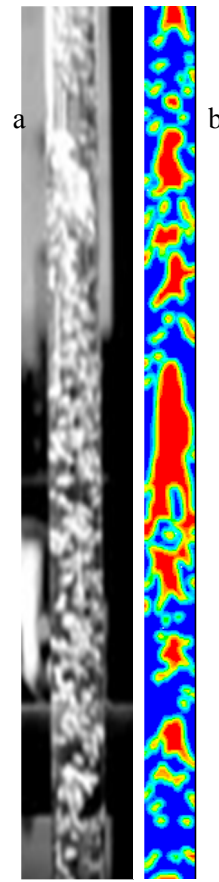


Figure: 4.6: Validation of Slug-Churn Flow, (a) slug-churn flow from [Kassab et al. \(2008\)](#), (b) Simulation result for slug flow at time $t = 1$ sec where AMFR is 0.033 kg/sec

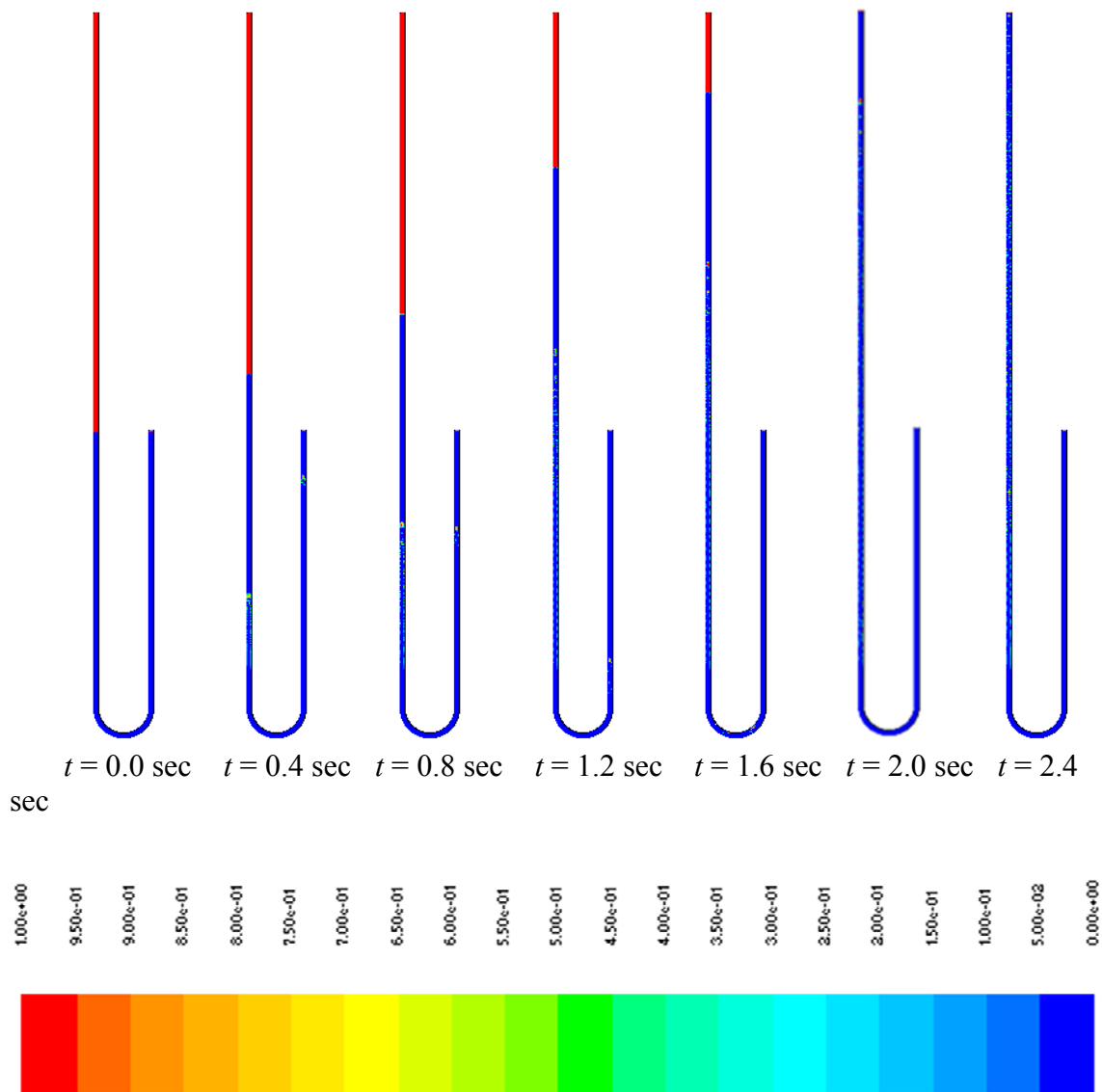
Since, the flow regimes obtained from numerical simulation is similar to that obtained experimentally. Hence, Validation was successful.

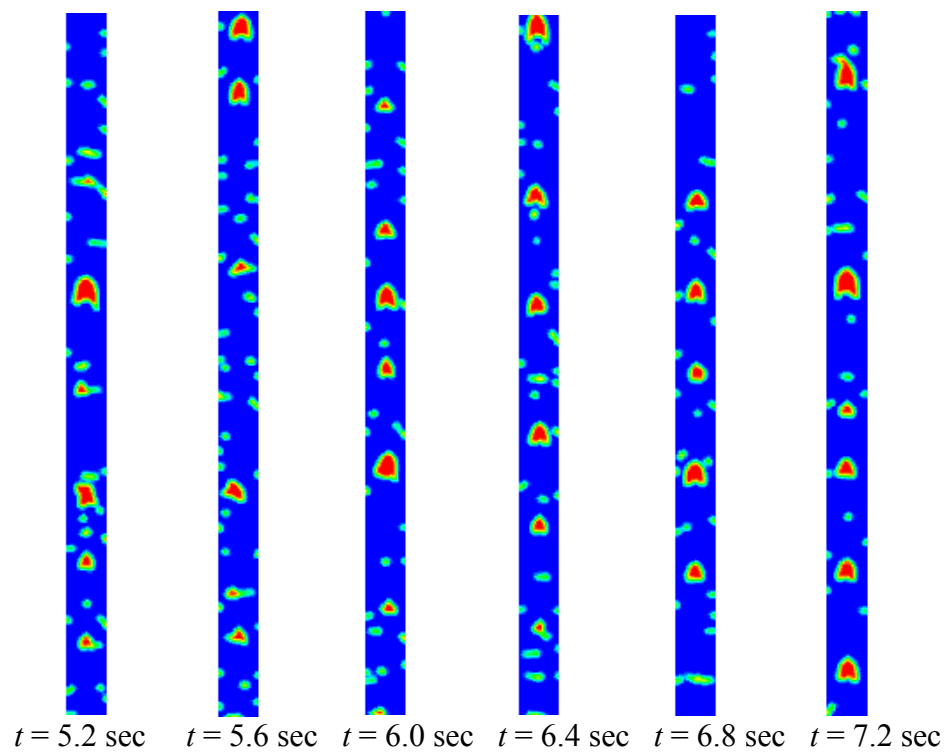
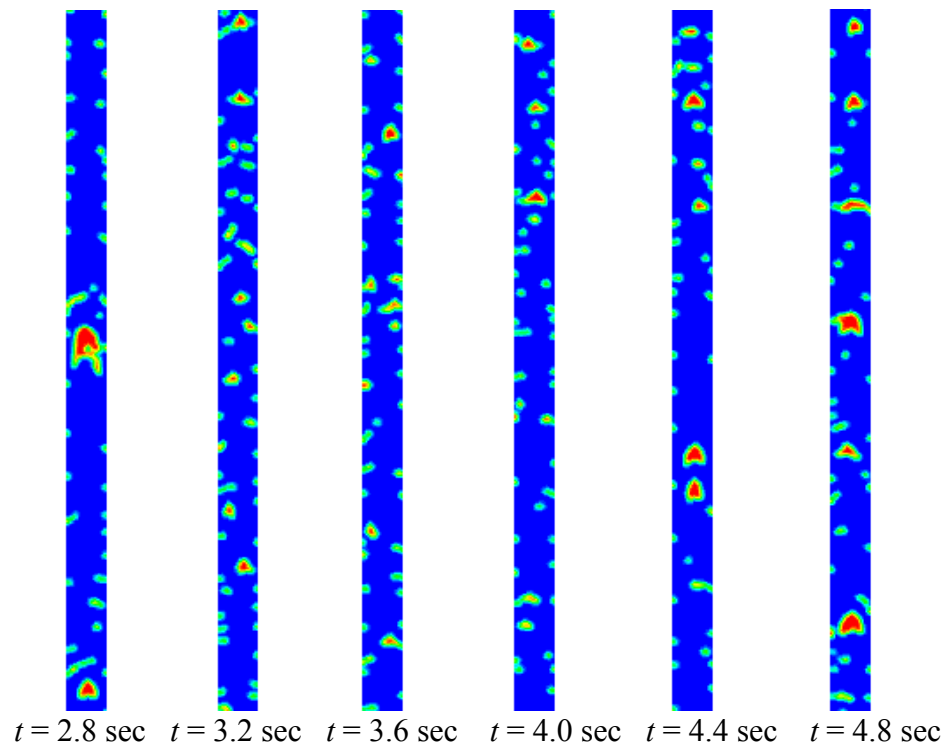
4.3 EFFECT OF AIR MASS FLOW RATE ON THE PHENOMENON

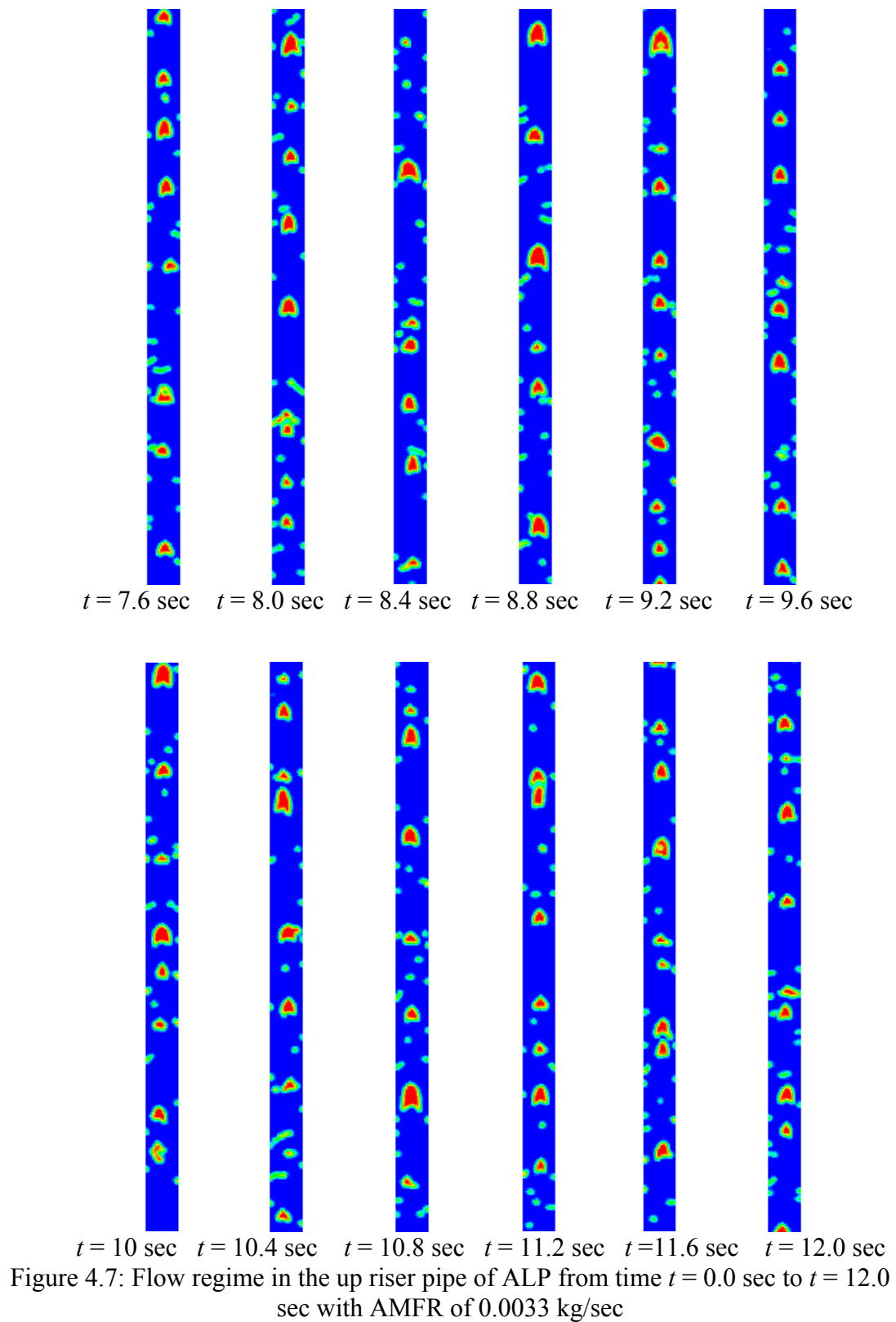
In this section, an attempt has been made to get the effect of AMFR on flow regime, velocity of air bubble moving in the upward direction and water mass flow rate at the outlet.

4.3.1 Effect of Air Mass Flow Rate on Flow Regimes: Basically, four different types of flow regimes is usually encountered in the study of flow regime of ALP. Either these four or combination of these four (occurs when there is a transition from one phase to another phase) may occur. One of them is bubbly-flow. As the name suggests, gaseous medium gets dispersed in continuous liquid phase and appears in the form of bubbles. Next is the slug-flow which is characterized by the appearance of axisymmetric bullet shaped large bubbles called “Taylor Bubble” which occurs in an intermittent manner. The third is churn-flow that occurs due to formation of vortex in sluggish flow regime which distorts the slugs leading to the formation of churns. Last it is the annular flow regime, where gaseous churns collide with one another, and thus, pushes liquid towards the wall and gases combine to form a channel. Section below discusses the various kinds of flow regime obtained in the present study by varying AMFR. Here, basically three flow regimes have been observed namely bubbly, slug and churn.

4.3.1.1 Case (i): Air Inlet Mass Flow Rate: 0.0033 kg/sec: Here, the flow regime (flow structure) have been captured with time by considering the AMFR = 0.0033 kg/sec. The phase contour at different time step have been shown below in Figure 4.7.



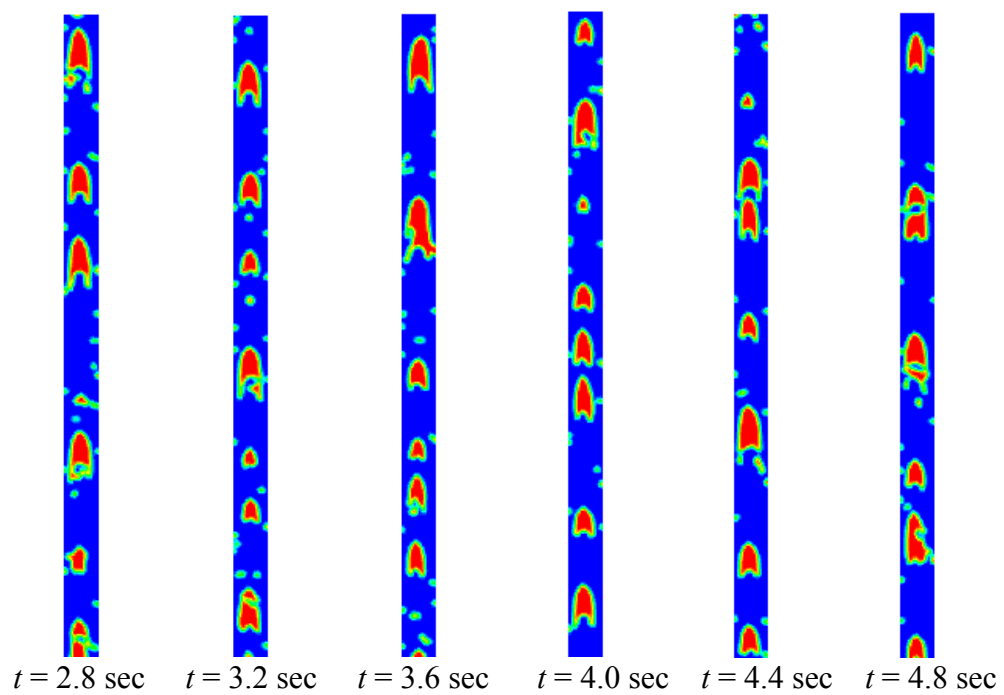
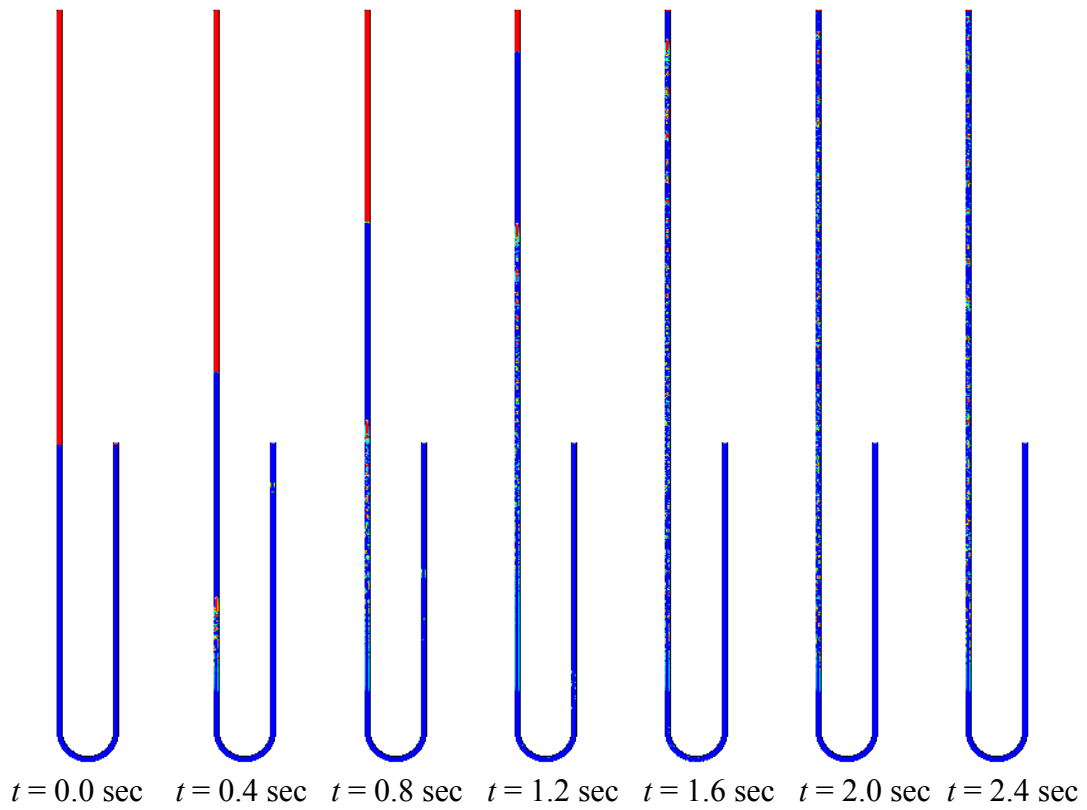


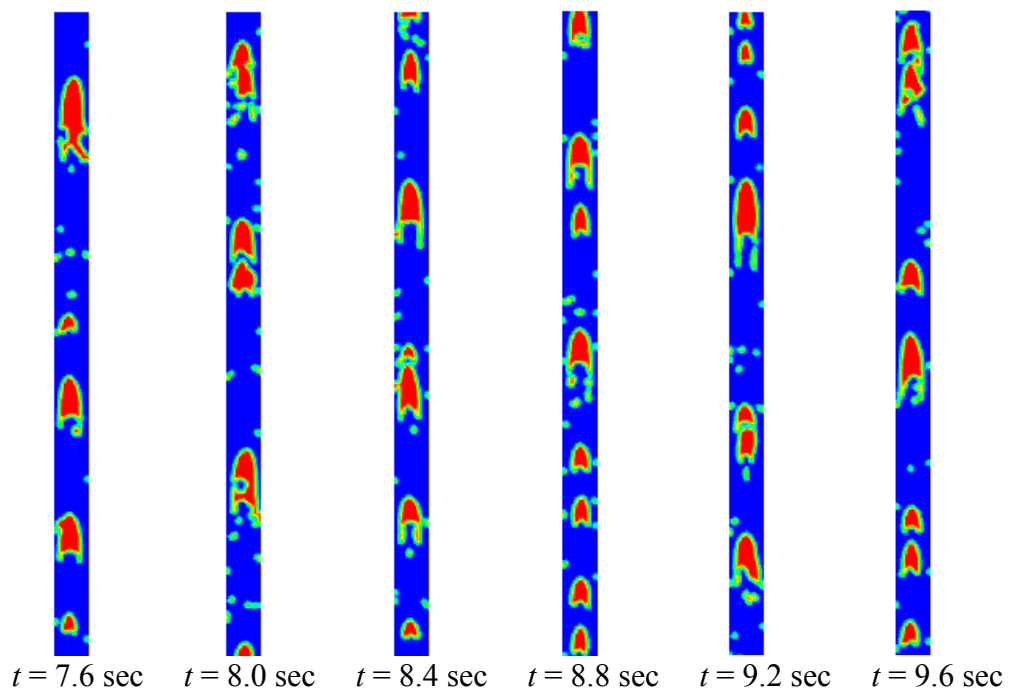
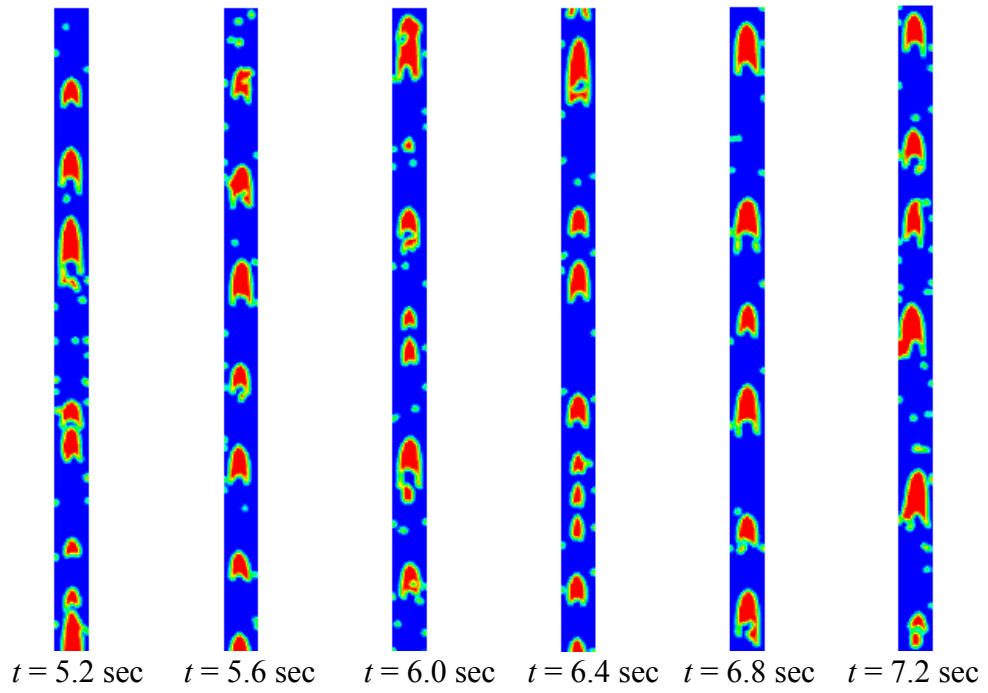


At time $t = 0.4 \text{ sec}$, bubbles of air start to form and move in the upward direction from the air inlet port. As time passes, the size of bubbles increases and it eventually

forms slugs. The bubbles moving in the upward direction, merge together and form a Taylor bubble (which is characteristic of slug flow). It can be observed that the formation of a Taylor bubble does not start at the beginning that is time $t = 0.0$, rather it takes some time. For AMFR = 0.0033 kg/s, Taylor bubble forms at time $t = 2.2$ sec. So, it can be concluded that a finite amount of time is required for the formation of bubble and therefore for the establishment of flow regime. To get the fully developed slug flow it will take some time as can be seen from Figure 4.7 (from $t = 2.8$ sec to $t = 6.8$ sec). The sequential occurrence of Taylor bubble is probably due to the time delay required to charge an adequate quantity of air to lift ample amount of water. Eventually as time passes, a steady state slug flow will be achieved.

4.3.1.2 Case (ii): Air Inlet Mass Flow Rate: 0.0110 kg/sec: Here, the flow regime (flow structure) have been captured with time by considering the AMFR = 0.011 kg/sec. The phase contour at different time step have been shown below in Figure 4.8. The results are shown from initial state at time $t = 0.0$ sec to $t = 12.0$ sec by setting the AMFR to 0.011 kg/sec. From Figure 4.8, it can be observed that unlike the previous case, here due to higher AMFR, the air entering from symmetrical inlets collide with each other and form a sluggish flow fluid with a very higher number of bubbles. Formation of a Taylor bubble does not start at the beginning that is time $t = 0.0$, rather it takes some time. For AMFR = 0.011 kg/s, Taylor bubble forms at time $t = 0.6$ sec. So, it can be concluded that a finite amount of time is required for the formation of bubble and therefore for the establishment of flow regime.





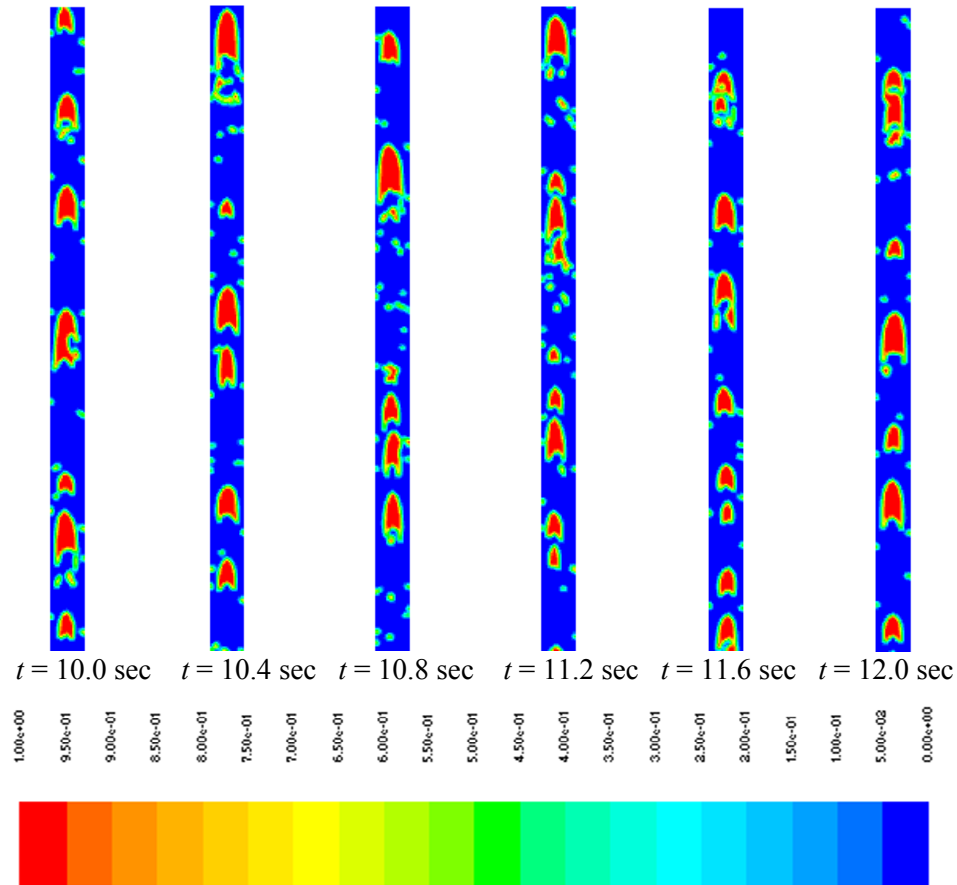
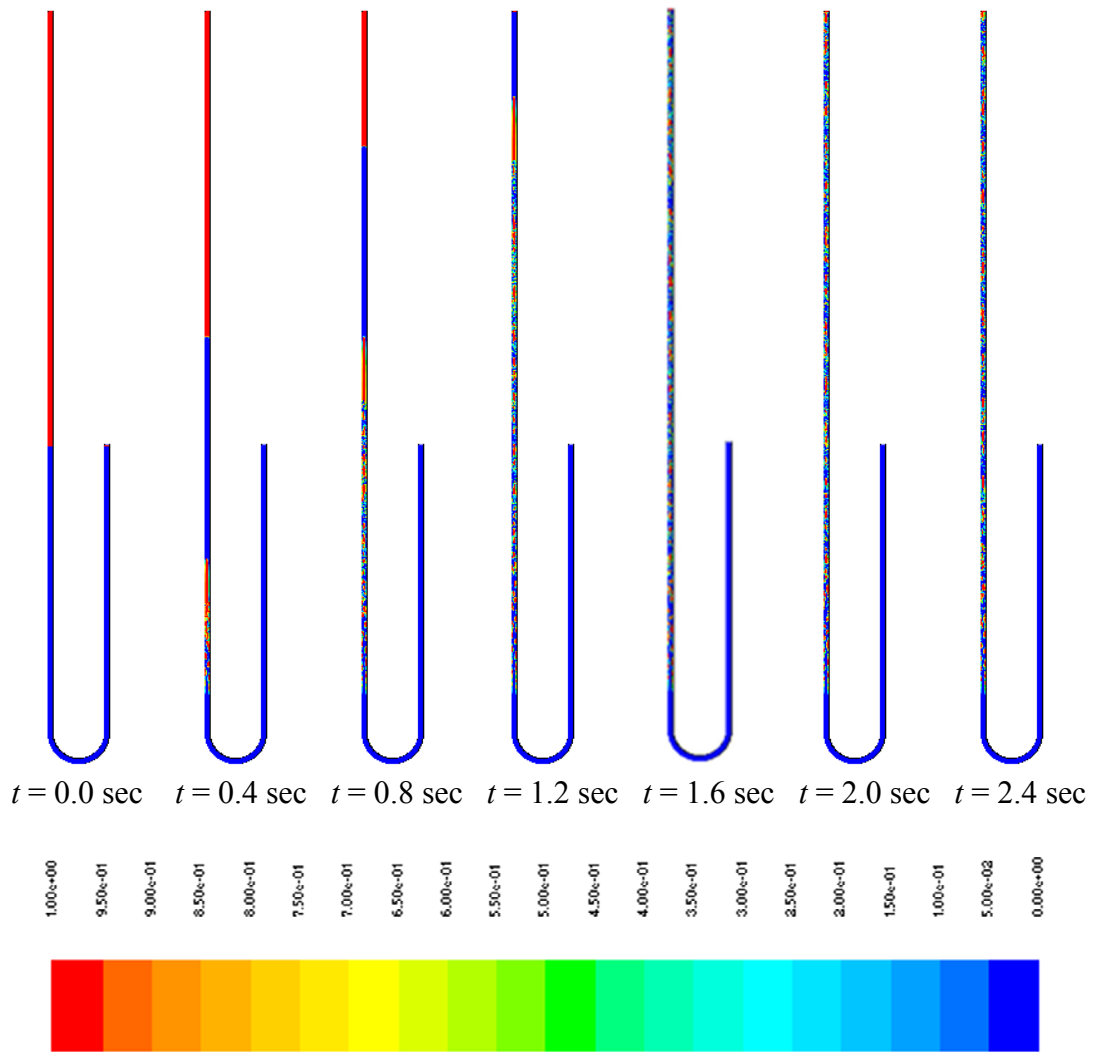
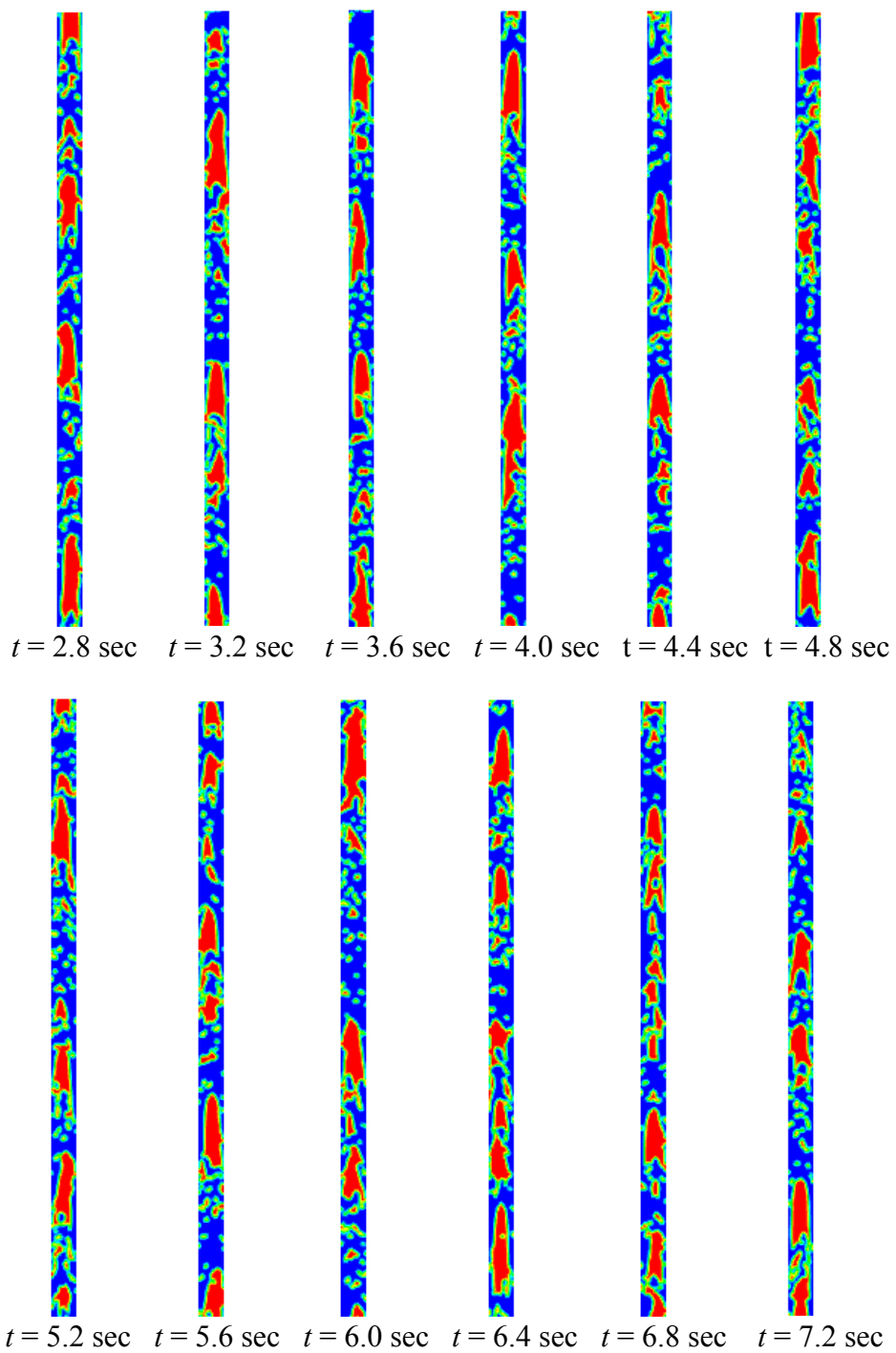


Figure 4.8: Flow regime in the up riser pipe of ALP from time $t = 0.0$ sec to $t = 12.0$ sec with AMFR of 0.011 kg/sec

Here, the pattern of slug flow is continuously changing with time. As time goes on number of Taylor bubbles is increasing as can be seen from Figure 4.8. But, it does not remain sustained for a longer period as shown in Figure 4.8. As the air bubble moves up, the thin water film directly in contact moves with it in the upward direction. As a result, the aerated water (aerated because presence of air reduces its specific gravity) in between two consecutive Taylor bubble moves in upward direction. This causes chaotic motion and due to this shape of Taylor bubble is distorted.

4.3.1.3 Case (iii): Air Inlet Mass Flow Rate: 0.0330 kg/sec: Here, the flow regime (flow structure) have been captured with time by considering the AMFR = 0.033 kg/sec. The phase contour at different time step have been shown below in Figure 4.9 from the initial state at time $t = 0.0$ sec to $t = 12.0$ sec.





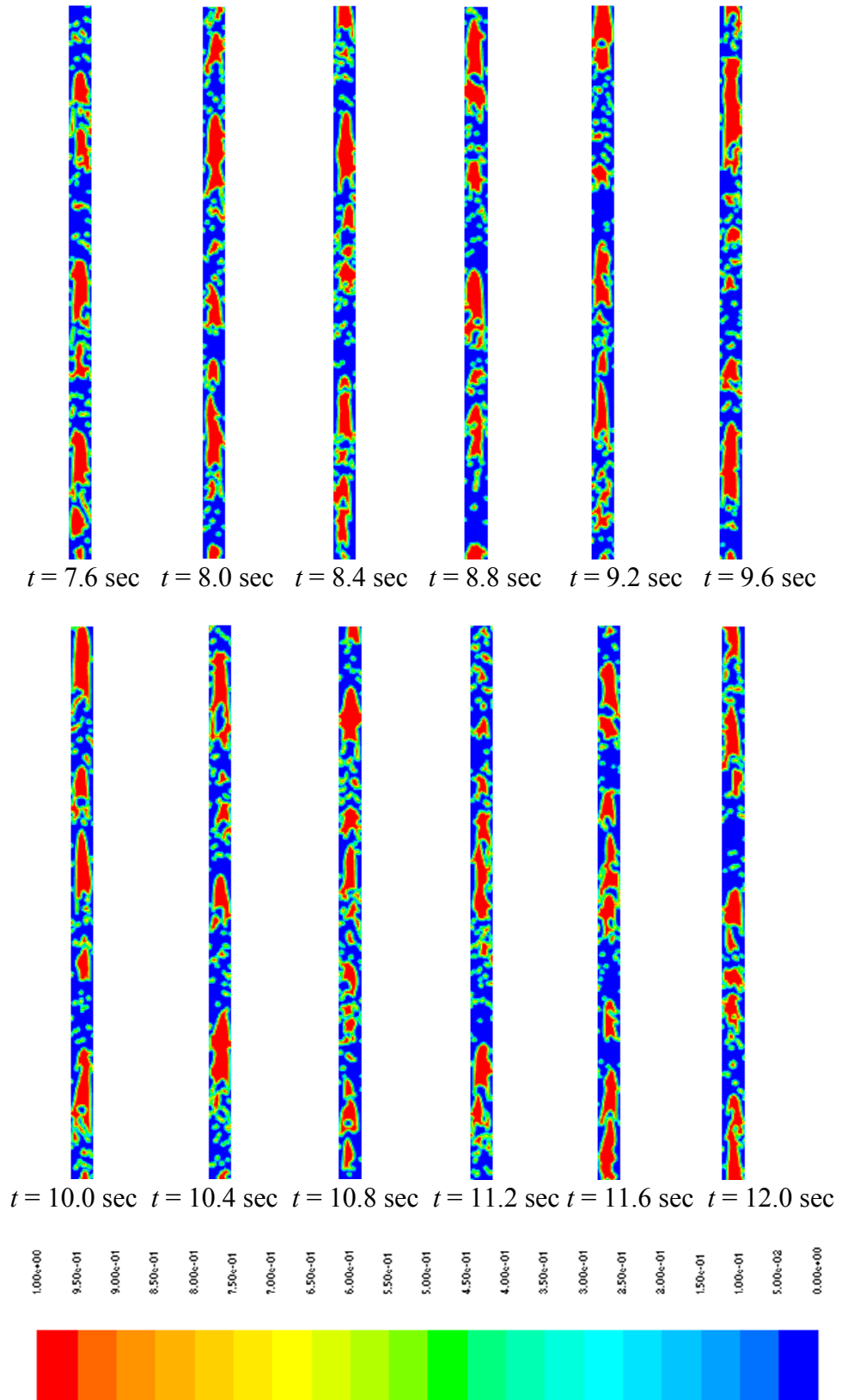
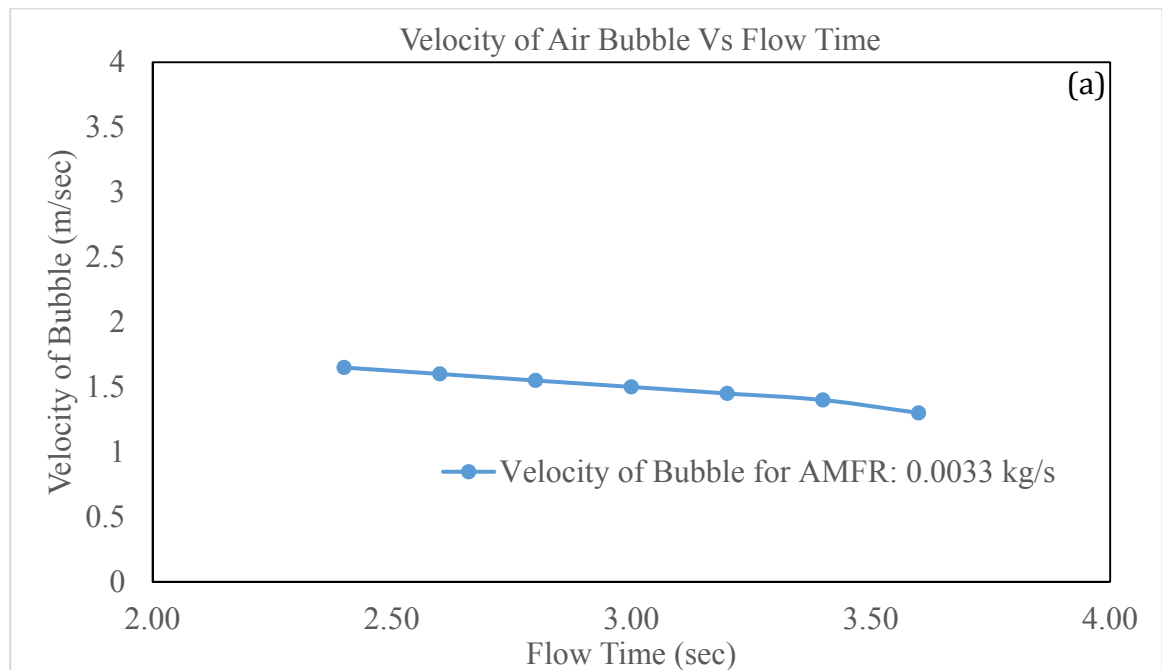


Figure 4.9: Flow regime in the up riser pipe of ALP from time $t = 0.0$ sec to $t = 12.0$ sec with AMFR of 0.033 kg/sec

As the mass flow rate is high, initially a large amount of air gets collected in the up-riser (for $t = 0.2$ sec) pipe. Formation of a bubble does not start at the beginning that is time $t = 0.0$, rather it takes some time. For AMFR = 0.033kg/s, it starts at time $t = 0.6$ s. So, it can be concluded that a finite amount of time is required for the formation of bubble and therefore for the establishment of flow regime. Later on the air forms a large Taylor bubble and thus lifts a large amount of water. Taylor bubble then gets distorted giving rise to a slug- churn flow regime ($t = 0.6$ to $t = 0.8$). At about time $t = 1.2$ sec water-air mixture reaches the top of up-riser pipe. The cycle of slug and slug-churn flow regime is repeated thereafter ($t = 1.2$ sec to $t = 12.0$ sec). It is evident that a maximum water flow rate can be obtained in slug-churn flow regime. It is due to the fact that here buoyancy forces as well as aerating phenomenon uplifts air-water mixture.

4.3.2 Effect of Air Mass Flow Rate on the Bubble Velocity: In this section, the influence of AMFR on bubble velocity is being depicted graphically.



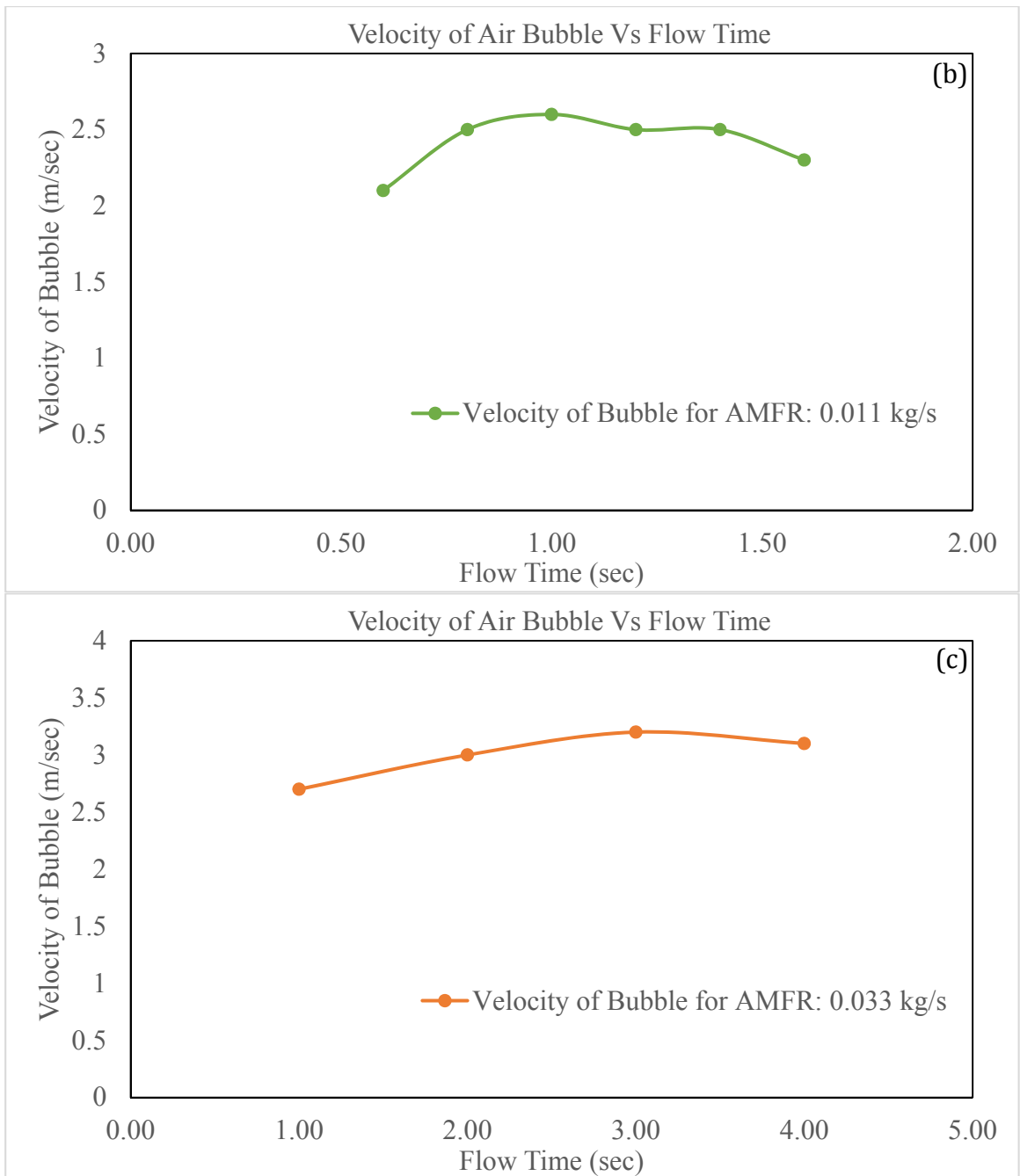


Figure 4.10: Variation of bubble velocity with flow time for different air mass flow rate. (a) AMFR = 0.0033 kg/sec. (b) AMFR = 0.011 kg/sec. (c) AMFR = 0.033 kg/sec.

The Figure 4.10 shows how the velocity of air bubble varies with time for different inlet AMFR separately. An air bubble while moving up also drags the water adjacent with interface. From the bubble velocity one can get the overall idea about the

velocity of mixture adjacent to the bubble. The bubble velocity at the instant $t + \Delta t$ can be calculated as

$$V_{t+\Delta t} = \frac{y_{t+\Delta t} - y_t}{\Delta t} \quad (4.1)$$

Here, $\Delta t = 0.2$ seconds. From the Figure 4.10, it is clear that average velocity of the bubble increases with the AMFR. It simply implies that time required (time span) to cover the distance of riser pipe is minimum when the AMFR is maximum. With increase in AMFR, the maximum bubble's velocity also increases. For instance, at AMFR = 0.0033 kg/s the maximum bubble velocity equal to 1.65 m/s whereas, for AMFR = 0.011kg/s its equal to 2.6 m/s and is maximum (3.2 m/s) for AMFR = 0.033 kg/s. A common trend can be observed from all the three figures that initially bubble velocity increases, reaches its maximum value and then decreases. It may be due to fact that water is lifted against gravity. The adhesive force from the pipe wall may also be responsible for this fact.

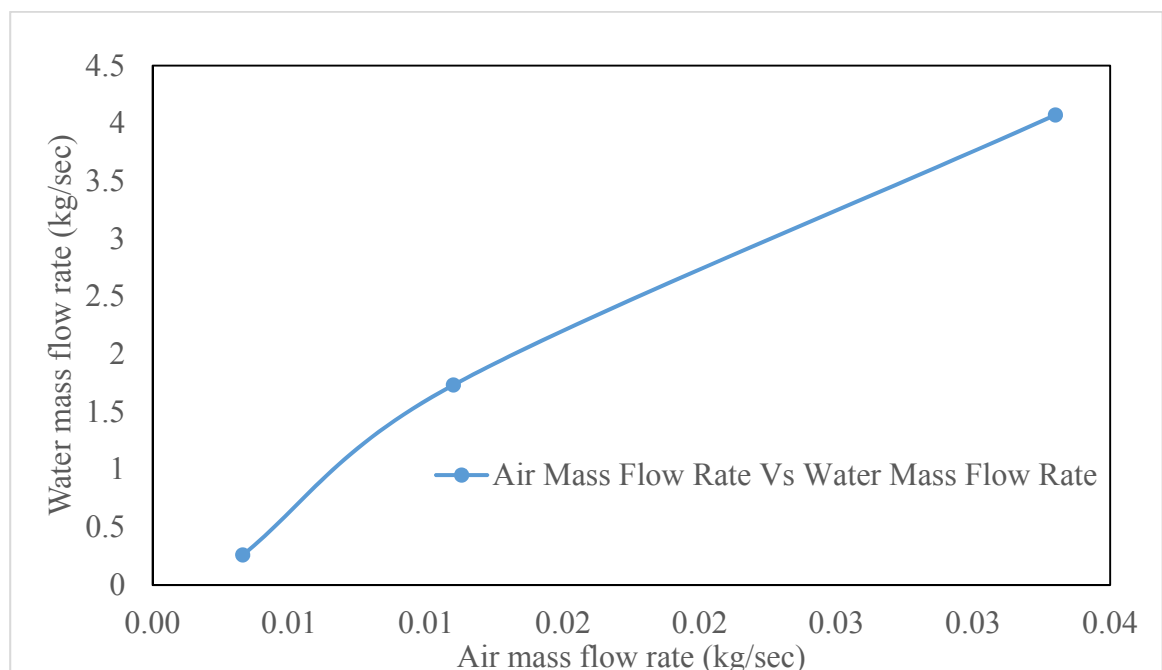


Figure 4.11: Variation of AMFR with water mass flow rate at submergence ratio = 0.4

4.3.3 Effect of Air Mass Flow Rate on Water Mass Flow rate at Exit: In this section, the influence of AMFR on the Water Mass Flow Rate at the outlet is discussed. Figure 4.11 shows this dependency. As can be seen from the Figure 4.11, the water mass flow rate increases with the rise in AMFR. For AMFR = 0.0033 kg/sec, the flow regime obtained was mostly bubbly in nature. Whereas, the flow regime obtained for AMFR = 0.011 kg/sec was sluggish. And, for AMFR = 0.033 kg/sec, the flow regime was mostly slug-churn mixture. So, it can be concluded that a maximum water mass flow rate at the exit is achieved for slug-churn flow regime.

CHAPTER 5:

CONCLUSION

AND

SCOPE OF FUTURE

WORK

5.1 CONCLUSION

This section describe the important finding obtained through the present study. All the major observations and the conclusion drawn from the different case studies are presented here in a condensed form. It should be noted that the following conclusion are only applicable for a small diameter up-riser pipe.

- Volume of Fluid (VOF) model with Finite Volume Method (FVM) can be used successfully to simulate and study the models related to two-phase flow in an air-lift pump.
- The air-lift pump with air-water two-phase flow can give the optimum performance (can lift optimum amount of water) when it runs with slug or slug-churn flow regime.
- Slug and slug-churn flow regime is observed when the air inlet mass flow rate is high. Again, the performance of the pump is optimum, when the flow structure is slug or slug-churn. Keeping this in mind one can say, if we increase the AMFR then, water flow rate at the outlet also increases when the submergence ratio is constant.
- At small values of mass flow rate, no up-liftment of water takes place as buoyancy force applied by air is not sufficient to raise water.

5.2 SCOPE OF FUTURE WORK

In this section the further research work that could be conducted in this field has been discussed.

- 1) In near future, somebody can study the effect of increment in the diameter of up-riser pipe on the performance of pump, water flow rate at the outlet and flow structure.
- 2) In future, someone can study the effect of the submergence ratio on the efficiency, water flow rate at outlet and flow regime by changing the length of the riser pipe.

REFERENCES

- Bergeles, A. E., 1949. Flow of gas-liquid mixture. *Chemical Engineering*, 104-106.
- Stenning, A. H., Martin, C. B., 1968. An analytical and experimental study of air-lift pump performance. *Journal of Engineering for Power* 90, 106–110.
- Sharma, N. D., Sachdeva, M. M., 1976. An air-lift pump performance study. *American Institute of Chemical Engineers Journal* 32, 61–64.
- DeCachard, F., Delhaye, J. M., 1996. A slug-churn flow model for small diameter air-lift pumps. *International Journal of Multiphase Flow* 22, 627–649.
- Khalil, M.F., Mansour, H., 1990. Improvement of the performance of an air-lift pump by means of surfactants. *Mansoura Engineering Journal* 15(2), 119-129.
- Iguchi, M., Terauchi, Y., 2001. Boundaries among bubbly and slug flow regimes in air–water two-phase flows in vertical pipe of poor wettability. *International Journal of Multiphase Flow* 27, 729–735.
- Furukawa, T., Fukano, T., 2001. Effects of liquid viscosity on flow patterns in vertical upward gas–liquid two-phase flow. *International Journal of Multiphase Flow* 27, 1109–1126.
- Hitoshi, F., Satoshi, O., Hirohiko, T., 2003. Operation performance of a small airlift pump for conveying solid particles. *Journal of Energy Resources Technology* 125, 17–25.
- White, E. T., Beardmore, R. H., 1962. The velocity of rise of single cylindrical air bubbles through liquids contained in vertical tubes. *Chemical Engineering Science* 17, 351-361.
- Zukoski, E. E., 1966. Influence of viscosity, surface tension, and inclination angle on motion of long bubbles in closed tubes, *Journal of Fluid Mechanics* 20, 821-832.

- Stapanoff, A. J., 1929. Thermodynamic theory of air-lift pump. American Society of Mechanical Engineers Journal 51, 49–55.
- Nicklin, D. J., 1963. The air-lift pump theory and optimization. Transactions of the Institution of Chemical Engineers 41, 29–39.
- Hanafizdeh, P., Saidi, M. H., Zarimi, A., Karimi, A., 2009. Effect of bubble size and angle of tapered upriser pipe on the effectiveness of a two phase lifting pump. Fluids Engineering Division Summer Meeting, ASME, 807-814.
- Hanafizdeh, P., Saidi, M. H., Moezzi M., 2014. Simulation of gas-liquid two phase flow in upriser pipe of gas-lift systems. Energy Equipment and Systems 2, 25-41.
- Kassab, S. K., Kandil, H. A., Warda, H. A., Ahmed, W. H., 2008. Air-lift pumps characteristics under two-phase flow conditions. International Journal of Heat and Fluid Flow 30(1), 88-98.